

NGC 1052 – A study of the pc-scale twin jet

M. Kadler, E. Ros, J. A. Zensus, A. P. Lobanov and H. Falcke

*Max-Planck-Institut für Radioastronomie, Auf dem Hügel 69, D-53121
Bonn, Germany, mkadler@mpifr-bonn.mpg.de*

Abstract. We present results of a VLBA multi-frequency study of the pc-scale twin jet in NGC 1052. We observed this object at epoch 1998.99 with the VLBA at 5, 8.4, 22 and 43 GHz both in total and linearly polarized intensity. The spectral analysis confirms the necessity of a free-free absorbing medium, obscuring the innermost part of both jets. At 5 GHz we found a compact linearly polarized emission region at the base of the eastern jet with a degree of polarization of 1.5%. At higher frequencies there is no evidence for polarization in our data. A core shift analysis constrains the position of the central engine to ~ 0.03 pc. The shift rates of the apparent core position with frequency confirm the strong influence of free-free absorption in conjunction with steep pressure gradients at the bases of both jets.

Introduction: NGC 1052 is a nearby elliptical galaxy that harbors an active galactic nucleus in its center. Its radio structure ranges from $\sim 20''$ down to the smallest resolvable scales below 1 milliarcsecond. Its bright compact radio core and its small distance of $D = 22.6$ Mpc makes NGC 1052 a prime target for VLBI studies of the environment of the central engine believed to be a supermassive black hole of about $10^{8\pm 1} M_{\odot}$.

On VLBI scales NGC 1052 shows a jet/counter-jet structure oriented at a position angle of about 65° . Kinematical studies at 15 GHz [1] show that the two jets are oriented close to the plane of the sky. The distribution of water maser emission in NGC 1052 on pc-scales was imaged with VLBI by [2]. The maser emission is concentrated in two groups of unresolved maser spots, lying along the western jet. Strong free-free absorption at the corresponding region of the source was found by [3] (see also [4]). The presence of atomic gas at the center of NGC 1052 is evident from HI absorption observations [3] and the X-ray spectrum of the nucleus [5].

Imaging and model fitting: In Fig. 1 we present VLBA images of NGC 1052 in total intensity at 5, 8.4, 22 and 43 GHz obtained from our observations on

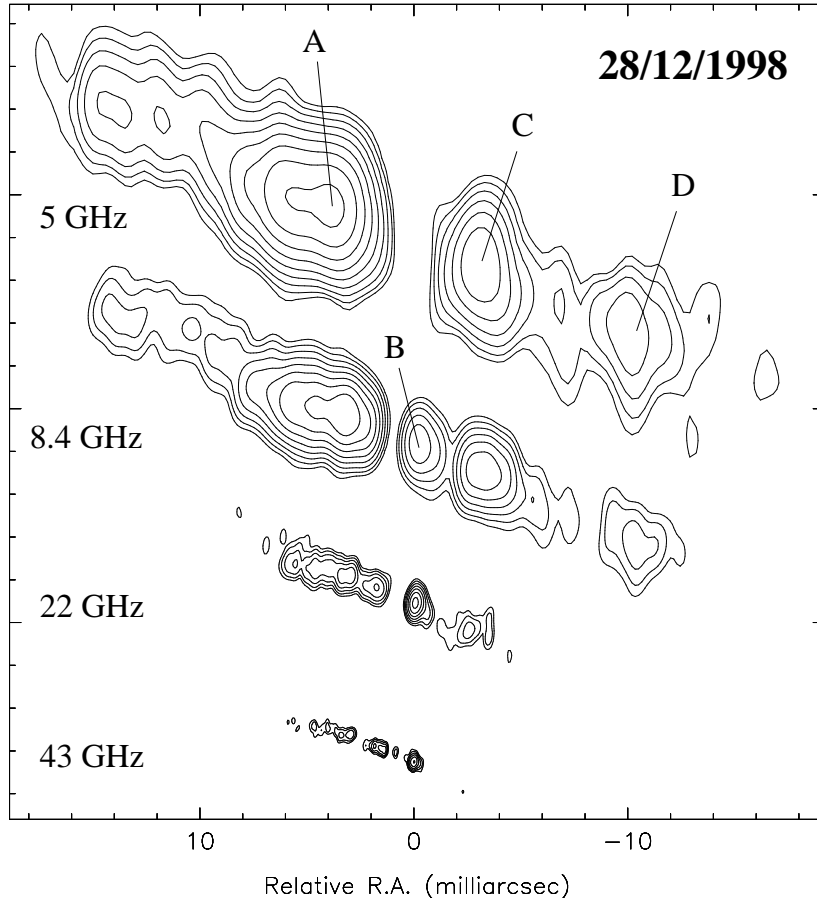


Figure 1. VLBA images of NGC 1052 at 5, 8.4, 22 and 43 GHz. The map parameters are given in Table 1.

December 28th 1998 (related parameters in Table 1). The images have been produced following standard procedures. In the images we define four regions, A (eastern jet), B, C and D (western jet). The alignment of the images at the four frequencies was performed through a pairwise identification of Gaussian model fit components between adjacent frequencies. We derived spectra (shown in Fig. 2) of the different regions of jet and counter-jet separately, by adding up the flux densities of the corresponding model components.

Both the eastern and the western jet have a steep spectrum at the highest frequencies. At low to intermediate frequencies the eastern jet remains steep between 22 and 8.4 GHz and becomes flat between 8.4 and 5 GHz whilst the western jet exhibits a turnover of its spectrum below 22 GHz. The innermost part of the western jet (region B) has a highly inverted spectrum. No emission is detectable in this region at 5 GHz, making the spectral index α ($S \propto \nu^{+\alpha}$) larger than 3. This value exceeds the theoretical maximal value of 2.5 for synchrotron

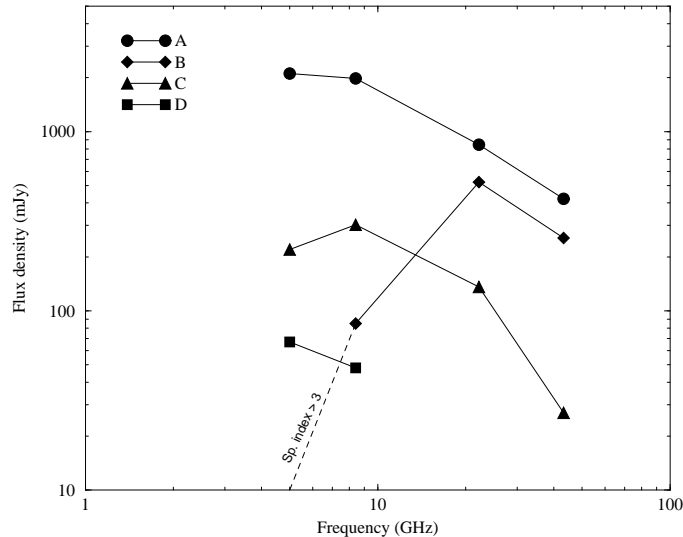


Figure 2. Spectra of the four source regions (A, B, C and D in Fig. 1), obtained from the model fitting of the visibility data.

self-absorption (see e.g. [6]) marking a possible region of external absorption (in an obscuring torus?) at the base of the western jet.

Polarimetry: We carried out a polarimetric imaging analysis following standard procedures (see [7]). We detected linearly polarized emission above a 3σ level only at 5 GHz. At this frequency, we found a compact region of linearly polarized emission at the base of the eastern jet, with a flux density of about 3 mJy beam^{-1} . This corresponds to a degree of polarization of 1.5%. The electric field vectors are parallel to the jet axis, i.e. the corresponding emission region is dominated by a magnetic field perpendicular to the jet axis (assuming no Faraday rotation). Our spectral measurements indicate that the emission from this part of the eastern jet is optically thick at 5 GHz. This implies that the polarized flux should increase at higher frequencies, a trend that we do not observe in our

Table 1. Map parameters for Fig. 1.

ν [Hz]	λ [cm]	beam [mas \times mas, $^\circ$]	S_{peak} [Jy/beam]	$S_{\text{tot}}^{(a)}$ [Jy]	rms [mJy/beam]	Contours [mJy/beam]
5	6	3.30×1.31 , -3.74	0.660^b	2.41	0.26	$0.99 \times (2,4,\dots,256,512)$
8.4	4	1.98×0.81 , -3.87	0.538^b	2.39	0.25	$0.81 \times (2,4,\dots,256,512)$
22	1.3	0.86×0.32 , -7.63	0.339^c	1.51	1.20	$1.02 \times (2,4,\dots,128,256)$
43	0.7	0.45×0.16 , -7.93	0.126^c	0.67	0.67	$1.89 \times (2,4,\dots,16,32,64)$

^a Total flux density recovered in the map model; ^b Corresponds to the A component; ^c Corresponds to the B component.

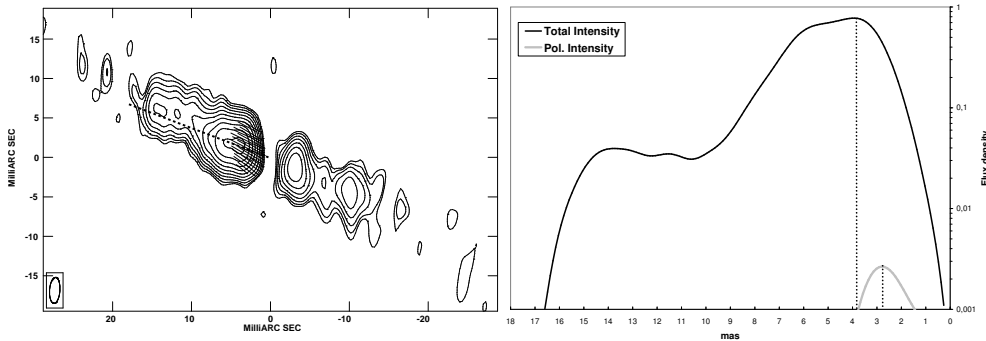


Figure 3. Left panel: 5 GHz image of the total intensity (contours) and the linearly polarized emission (segments representing the EVPA, proportional to the flux density). Right panel: profile (dashed line in the left panel) of the total and linearly polarized intensity at 5 GHz taken along P.A.= 69°.

data. This can be interpreted as an effect of optical depth: if the jet is linearly polarized only in the outer layers, no linearly polarized emission is expected at high frequencies where the radiation originates in deeper layers of the jet, closer to the geometrical jet axis.

Core-shift analysis: The symmetry between the jet and the counter-jet constrains the position of the central engine in NGC 1052. The location where a jet becomes visible at a given frequency is usually referred to as the “core”. The core is located at the distance to the central engine r_c , where the optical depth τ has fallen to be ~ 1 . This distance is given by: $r_c \sim \nu^{-\frac{1}{k_r}}$, where $k_r = ((3 - 2\alpha)m + 2n - 2)/(5 - 2\alpha)$, with m and n the power indices of the magnetic field and the particle density: $B \sim r^{-m}$, $N \sim r^{-n}$ [8]. Measuring r_c at two frequencies allows one to determine k_r in the corresponding region of the jet. For a freely expanding jet in equipartition [9], $k_r=1$. The value of k_r is larger in regions with steep pressure gradients and may reach 2.5, for reasonable values of m, n (≤ 4 , see [8]). If external absorption determines the apparent core position, comparable density gradients of the external medium can alter k_r to values above 2.5.

The values of k_r deduced depend crucially on the absolute values of r_c on the two sides and therefore on the assumed position of the central engine. Four scenarios have been tested with different reference points (see Fig. 4). Table 2 gives the derived values of k_r for each scenario. The area between the model components A 15 and B 2b is the most likely location of the central engine and the center between both components is a natural choice for its exact position (scenario 1). Shifting the reference point eastwards (scenarios 2 and 3) alters the values of k_r into unphysically large regimes (requiring density gradients $\propto r^{-10}$ and higher).

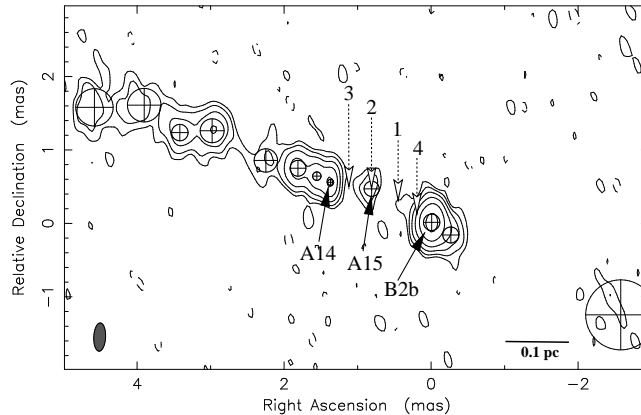


Figure 4. Image with the model fitting results of the 43 GHz data. The circles represent the Gaussian components. The innermost jet components are labeled as A 14, A 15 and B 2b. The putative locations of the central engine are indicated (dashed arrows) for 4 different scenarios (see discussion in the text).

Assuming the true center of activity to be located more westwards (closer to B 2b, scenario 4), the values of k_r derived are still acceptable. We show the core positions of both jets at the different frequencies for the first case (scenario 1) in Fig. 5. The eastern jet has rather high values of k_r below 22 GHz, although still in agreement with steep pressure gradients in the jet environment. Above 22 GHz k_r is 3.9 ± 0.8 , which is a good indicator for free-free absorption affecting the jet opacity. The western jet has values of k_r as high as 6.8 ± 2.7 between 22 and 43 GHz, suggesting a large contribution from free-free absorption.

Our results from the core-shift analysis support the picture of a free-free absorbing torus covering mainly the inner part of the western jet and also a smaller fraction of the eastern jet. The true center of activity in NGC 1052 can be determined to lie between the model components A 15 and B 2b, with an uncertainty of only ~ 0.03 pc.

Acknowledgments. We want to thank A. Tarchi for his valuable help. The VLBA is operated by the National Radio Astronomy Observatory (NRAO), a fa-

Table 2. k_r values for the four different putative centers of activity.

ν [GHz]	—Scenario 1—		—Scenario 2—		—Scenario 3—		—Scenario 4—	
	$k_{r,east}$	$k_{r,west}$	$k_{r,east}$	$k_{r,west}$	$k_{r,east}$	$k_{r,west}$	$k_{r,east}$	$k_{r,west}$
5–8.4	3.1 ± 2.6	–	2.5 ± 2.2	–	3.0 ± 3.6	–	3.4 ± 2.8	–
8.4–22	2.1 ± 0.5	6.6 ± 2.8	1.5 ± 0.3	11.9 ± 5.1	1.0 ± 0.2	14.8 ± 6.2	2.4 ± 0.6	3.8 ± 1.6
22–43	3.9 ± 0.8	6.8 ± 2.7	2.4 ± 0.5	13.0 ± 5.2	1.3 ± 0.2	17.1 ± 7.1	4.8 ± 1.0	3.6 ± 1.3

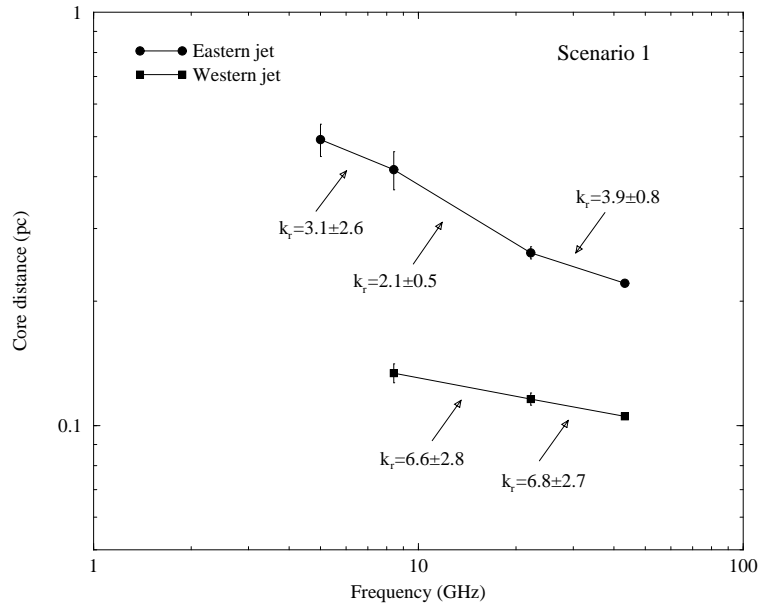


Figure 5. Core positions in the two jets at the different frequencies for scenario 1 (see Fig. 4). The corresponding values of k_r for the core shift between adjacent frequencies are labeled. Smaller core shifts correspond to higher values of k_r . Table 2 provides the values of k_r for the other three scenarios.

cility of the National Science Foundation operated under cooperative agreement by Associated Universities, Inc.

References

- [1] Vermeulen et al., A&A, in preparation
- [2] Claussen et al., 1998, ApJ 500, L129
- [3] Kellermann et al., 1999, BAAS 31, 856
- [4] Kameno et al., 2001, PASJ 53, 169
- [5] Weaver et al., 1999, ApJ 520, 130
- [6] Rybicki, G. B. & Lightman, A. P., Radiative Processes in Astrophysics, Wiley-Interscience, New York, 1979
- [7] Leppänen et al., 1995, AJ 100, 2479
- [8] Lobanov, A. P., 1998, A&A 330, 79
- [9] Blandford, R. D. & Königl, A., 1979, ApJ 232, 34